

# N-NITRO-L-ARGININE METHYL ESTER HYDROCHLORIDE INDUCED ENDOTHELIAL DYSFUNCTION AND ATHEROSCLEROSIS MODEL IN RATS

Muhammet Kursat Simsek<sup>1</sup>, Mustafa Mahmut Baris<sup>2</sup>, Osman Yilmaz<sup>3</sup>, Zekiye Sultan Altun<sup>4</sup>, Safiye Aktas<sup>4</sup>, Yasemin Cakir<sup>5</sup>, Sibel Buyukcoban<sup>6</sup>, Mustafa Secil<sup>2</sup>

<sup>1</sup> Merkezefendi State Hospital, Department of Radiology, Manisa, Turkey

<sup>2</sup> Faculty of Medicine, Department of Radiology, Dokuz Eylul University, Izmir, Turkey

<sup>3</sup> Vocational School of Health Services, Medical Services and Anesthesia Program, Dokuz Eylul University, Izmir, Turkey

<sup>4</sup> Institute of Health Sciences, Department of Basic Oncology, Dokuz Eylul University, Izmir, Turkey

<sup>5</sup> Dr. Behcet Uz Children's Education and Research Hospital, Department of Pathology, Izmir, Turkey

<sup>6</sup> Faculty of Medicine, Department of Anesthesiology and Reanimation, Dokuz Eylul University, Izmir, Turkey

ORCID: M.K.S. 0000-0002-9284-6999; M.M.B. 0000-0002-6496-2781; O.Y. 0000-0001-7817-7576; Z.S.A. 0000-0002-1558-4534; S.A. 0000-0002-7658-5565; Y.C. 0000-0002-1671-0635; S.B. 0000-0002-5756-980X; M.S. 0000-0001-7350-2202

**Corresponding author:** Muhammet Kursat Simsek, **E-mail:** dr.mksimsek@gmail.com

**Received:** 01.01.2023; **Accepted:** 13.06.2023; **Available Online Date:** 30.09.2023

©Copyright 2021 by Dokuz Eylül University, Institute of Health Sciences - Available online at <https://dergipark.org.tr/en/pub/jbachs>

**Cite this article as:** Simsek MK, Baris MM, Yilmaz O, Altun ZS, Aktas S, Cakir Y, Buyukcoban S, Secil M. N-Nitro-L-Arginine Methyl Ester Hydrochloride Induced Endothelial Dysfunction and Atherosclerosis Model in Rats. J Basic Clin Health Sci 2023; 7: 114-121.

## ABSTRACT

**Purpose:** Atherosclerosis (AS) related diseases are the most common causes of mortality worldwide. N-Nitro-L-Arginine Methyl Ester Hydrochloride (L-NAME)-induced endothelial dysfunction (ED) and AS models require invasive methods for diagnosis. We aimed to establish noninvasive ultrasonography (USG) model for evaluating ED and AS in rats.

**Material and Methods:** 23 Wistar Albino rats were divided into four groups. Right CCA (rCCA), left CCA (lCCA), abdominal aorta (AA), and right iliac artery (rIA) IMT values of all rats were measured at the beginning of the experiment and before sacrifice by USG. Right kidney RI values were calculated at similar times also. Histopathological and immunohistochemical analyzes were performed. In the sham group, rats received intraperitoneally (IP) sodium chloride. In the L-NAME groups, IP L-NAME was administered.

**Results:** In the early effect group, significant increase was found in IMT measurements compared to the sham group. In the late effect group, significant increase was found in IMT measurements compared to the sham group. In addition, rRI increased significantly in the group at the end of the experiment.

**Conclusion:** In small animal experiments which ED and AS were studied, a whole-body diagnostic noninvasive model was created for the first time with ultrasonography.

**Keywords:** Ultrasound, intima-media thickness, L-NAME, renal resistive index

## INTRODUCTION

Atherosclerosis (AS) and related cardiovascular diseases are the most common causes of mortality worldwide (1,2). Before clinical findings, changes

such as endothelial dysfunction (ED) and increased vascular intima-media thickness (IMT) occur in the vascular wall (3). Therefore, in addition to invasive methods such as coronary artery angiography,

**Table 1.** Study groups and the procedures

	Day 0	Day 1-7	Day 10	Day 28
Control (n=3)	USG + Blood Samples + Sacrification			
Sham (n=6)	USG + Blood Samples	2x1 IP SF	Follow up	USG + Blood Samples + Sacrification
EE (n=7)	USG + Blood Samples	2x1 IP L-NAME	USG + Blood Samples + Sacrification	
LE (n=7)	USG + Blood Samples	2x1 IP L-NAME	Follow up	USG + Blood Samples + Sacrification

USG: Ultrasound, IP: Intraperitonealy, SF: Isotonic saline, L-NAME: N-Nitro-L-Arginine Methyl Ester Hydrochloride, EE: Early effect, LE: Late effect

intravascular ultrasonography (USG), and optical coherence tomography, many noninvasive imaging methods such as common carotid artery (CCA) USG, computed tomography, magnetic resonance imaging, and scintigraphy are used in the diagnosis of AS (4). ED detected in peripheral arteries significantly correlates with coronary artery ED and angiographically proven coronary artery disease (5-7). In addition, patients with ED who do not have coronary artery disease angiographically have an increased risk of myocardial infarction, coronary revascularization, and cardiac death (8,9). Diagnosis of ED means detection of vascular disease in the asymptomatic stage. Therefore, it is an important marker for planning medical and invasive treatments (10). An increase in IMT in the coronary and peripheral artery walls have been found in adults and children with ED (11). In addition, many studies have shown that the increase in IMT is an excellent marker in diagnosing early-stage AS (12). For these reasons, carotid IMT increase is the most frequently used imaging method in daily routine in detecting AS in coronary arteries.

Mice, rats, hamsters, guinea pigs, and rabbits are frequently used in experimental ED and AS models (13). Rats are one of the most used species in these models. The rat ED model created with N-Nitro-L-Arginine Methyl Ester Hydrochloride is the preferred method in these studies (14,15). These N-Nitro-L-Arginine Methyl Ester Hydrochloride-induced ED models require invasive methods such as urine collection, blood collection, angiography, and sacrifice for diagnosis. Noninvasive approaches such as flow-mediated dilatation (FMD) and IMT measurement are also available to evaluate ED in

addition to these methods. FMD has limitations such as being dependent on user experience, requiring additional devices, and not being practical for daily routine. Also, it requires a prolonged period to perform the investigation.

On the other hand, IMT measurement is very practical, easy, and fast (16). The CCA and abdominal aorta (AA) are frequently used anatomical regions for IMT measurement. In the literature, IMT measurement in N-Nitro-L-Arginine Methyl Ester Hydrochloride-induced rat ED model has been defined in many anatomical areas of many studies (17,18). But no study performs IMT measurement without an invasive correlation method.

NO reduces renal vascular resistance. Renal resistive index (rRI) and cardiovascular diseases increase in hypertensive patients (19). Renal atherosclerosis and renal function correlate with rRI (20, 21, 22). No study focused on specific organ imaging for early detection of ED in N-Nitro-L-Arginine Methyl Ester Hydrochloride-induced rat models. This brings us to the following two questions; can IMT measurement be enough and accurate to show ED alone? What else can we evaluate with ultrasound to detect ED in N-Nitro-L-Arginine Methyl Ester Hydrochloride-induced rat models? In our study, we aimed to establish a noninvasive standard and practical USG model for evaluating ED in the N-Nitro-L-Arginine Methyl Ester Hydrochloride-induced endothelial dysfunction rat model.

**MATERIAL AND METHODS**

The Dokuz Eylul University Animal Care and Use Ethical Committee approved all animal protocols (Date: 14.07.2018. Number: 37 / 2018). ARRIVE

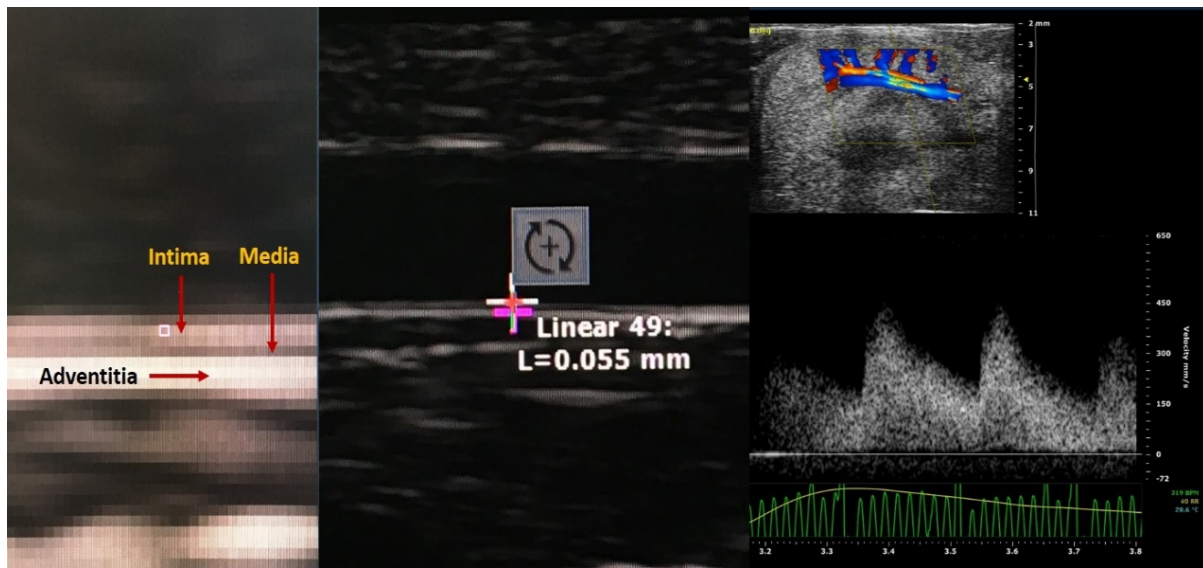


**Figure 1.** Ultrasonographic intima-media layers, measurement of these layers and renal resistive index

guidelines have been followed in this study. Using the Mann-Whitney U test, the minimum sample size was found to be twenty-one with a margin of error of 0.05 and a power of 0.80 and an effect size of 0.80.

Four to five weeks old 23 Wistar Albino female rats (300-350 g) were divided into four groups (control, sham, N-Nitro-L-Arginine Methyl Ester Hydrochloride early effect (EE), N-Nitro-L-Arginine Methyl Ester Hydrochloride late effect (LE)). Right CCA (rCCA), left CCA (lCCA), AA, and right iliac artery (rIA) IMT values of all rats were measured at the beginning of the experiment and before sacrifice by USG. In addition, histopathological (HP) and immunohistochemical (IHC) analyzes were performed on similar vessels and blood samples. Right kidney RI (rRI) values were calculated at similar times by USG also. All these procedures are shown in the table 1.

Three rats in the control group were used to evaluate the normal values of tissue thicknesses and organ measurements in the experiment. The rats in this group were sacrificed after USG measurements and tissue, and blood samples were collected. Sham group was created to compensate for stress variables such as aging and intraperitoneally (IP) injection in the experiments. In the sham group, six rats received IP 0.5mL of 0.09% sodium chloride (SC) twice a day for one week. After USG measurements, rats were sacrificed, and tissue and blood samples were collected on the 28<sup>th</sup> day.

The EE and LE groups had seven rats each. In these N-Nitro-L-Arginine Methyl Ester Hydrochloride-induced groups, IP 0.5mL 185 µM/kg N-Nitro-L-

Arginine Methyl Ester Hydrochloride was administered twice a day for a week. After the USG measurements, seven rats on the 10<sup>th</sup> day and the other seven on the 28<sup>th</sup> day of the experiment were sacrificed. In addition, tissue and blood samples were collected for HP and IHC analyzes.

General anesthesia with sevoflurane was applied with a sevoflurane vaporizer. Throughout the measurement procedures, the anesthesiologist adjusted the anesthetic agent levels if needed. The rats to be sacrificed after the measurement procedure was euthanized by sevoflurane inhalation anesthesia.

### Ultrasound Measurements

All ultrasonography evaluations were performed with Visual Sonics Vevo 2100 ultra-high frequency, high resolution, USG system designed for small animal studies (Fujifilm Visual Sonics, Inc. Toronto, Canada). All USG evaluations were performed by the MS550 (22-55 MHz) high-frequency linear probe. After selecting this probe, 'carotid' presets for CCA, AA, and IA, and 'general imaging' presets for kidneys were selected. In addition, the 'med flow' preset was chosen for kidney Doppler and spectral USG examinations, which is automatically suggested by the device.

Sevoflurane anesthetized rats were placed supine on the Vevo Imaging Station's small animal table for evaluation. The subjects' limbs were fixed to the appropriate places on the table where the sensors were on the table, and maintenance anesthesia was continued. A rectal thermometer was placed in rats,

**Table 2. Ultrasonographic and histopathological intima-media thickness and renal RI**

<b>ULTRASONOGRAPHIC INTIMA-MEDIA THICKNESS and RENAL RI</b>				
	Control	Sham	Early Effect	Late Effect
	Median (Min-Max)	Median (Min-Max)	Median (Min-Max)	Median (Min-Max)
Right CCA First Day (mm)	0,062 (0,056-0,063)	0,062 (0,058-0,067)	0,057 (0,055-0,061)	0,060 (0,055-0,062)
Right CCA Last Day (mm)	-	0,062 (0,055-0,066)	0,072 (0,069-0,072)	0,082 (0,075-0,090)
Left CCA First Day (mm)	0,060 (0,060-0,062)	0,062 (0,055-0,062)	0,060 (0,057-0,062)	0,062 (0,055-0,067)
Left CCA Last Day (mm)	-	0,062 (0,058-0,062)	0,070 (0,066-0,073)	0,082 (0,075-0,083)
AA First Day (mm)	0,082 (0,080-0,083)	0,075 (0,070-0,078)	0,075 (0,068-0,079)	0,069 (0,063-0,075)
AA Last Day (mm)	-	0,079 (0,075-0,083)	0,090 (0,077-0,098)	0,098 (0,085-0,110)
IA First Day (mm)	0,075 (0,071-0,080)	0,069 (0,067-0,076)	0,070 (0,062-0,076)	0,063 (0,055-0,070)
IA Last Day (mm)	-	0,070 (0,064-0,075)	0,083 (0,070-0,092)	0,090 (0,082-0,096)
Renal RI First Day	0,54 (0,54-0,057)	0,54 (0,43-0,58)	0,52 (0,44-0,57)	0,53 (0,47-0,55)
Renal RI Last Day	-	0,53 (0,43-0,60)	0,50 (0,45-0,55)	0,58 (0,50-0,64)
<b>HISTOPATHOLOGICAL INTIMATE-MEDIA THICKNESS</b>				
	Control	Sham	Early Effect	Late Effect
	Median (Min-Max)	Median (Min-Max)	Median (Min-Max)	Median (Min-Max)
Right CCA (mm)	0,044 (0,039-0,045)	0,049 (0,043-0,057)	0,056 (0,051-0,064)	0,059 (0,052-0,084)
Left CCA (mm)	0,037 (0,027-0,049)	0,045 (0,034-0,052)	0,057 (0,054-0,067)	0,053 (0,051-0,078)
AA (mm)	0,079 (0,065-0,082)	0,071 (0,068-0,087)	0,094 (0,074-0,105)	0,095 (0,083-0,128)
IA (mm)	0,065 (0,061-0,077)	0,058 (0,046-0,083)	0,085 (0,080-0,100)	0,088 (0,072-0,097)

RI: Resistive index, AA: Abdominal aorta, IA: Iliac artery

and the vital signs such as body temperature, respiration, and heart rate were monitored. Thanks to the fixation and attachment of the sensors, it was ensured that electrocardiography was recorded simultaneously with USG images. After the depilatory cream was applied to the abdomen and neck, rat hairs were cleaned, and USG measurements were started.

rCCA, ICCA, AA, rIA, and kidney tissues were scanned manually. The probe is positioned parallel to the long axis of the vessels. The vessel wall consists of three different echogenic surfaces. The first echogenic line between the vessel lumen and the vessel wall is the lumen-intima surface; the line between the hypoechoic media and hyperechoic adventitia layers was accepted as

the media-adventitia surface, and the measurement was made between these two surfaces (Figure 1). Ideally, for IMT measurements, images with the clearest view of the posterior wall of the artery were taken at the first millimeter (mm) before branching in CCA; first mm in the caudally from the exit of renal vessels in AA; and at the first mm level before branching in IA. In these localizations, if the best image could not be obtained due to inappropriate images containing artifacts or anatomical differences from rats, images were recorded from the region closest to the ideal area. The high-frequency probe is fixed with the help of the Vevo Imaging Station. Images were taken from the intrarenal level in the right kidney spectral measurements, preferably from the interlobar arteries. At least two series of images were taken from the defined regions. All video images were recorded for measurements. Three measurements were made from each series, and the average value of these three measurements was accepted as IMT and RI. Two radiologists (Practitioner 1 and Practitioner 2, respectively) performed all measurements with eight and three years of experience in laboratory animal imaging. To determine the reliability of the measurements among the practitioners, the end-of-experiment USG images of the sham and LE groups were measured and recorded separately by both practitioners at two weeks intervals. Interobserver reliability was evaluated statistically.

### Histopathologic Measurements

To confirm ED, endothelial nitric oxide synthase (eNOS), asymmetric dimethyl arginine (ADMA), and vascular endothelial growth factor (VEGF) levels were measured in plasma samples at the beginning and the end of the experiment. eNOS and endothelin 1 (ET1) levels were measured at the end of the experiment in rCCA, ICCA, AA, and rIA tissues to confirm the development of ED. Also, HP IMT measurements were performed at the end of the experiments for verification. All these measurements were made by a single pathologist with 8 years of experience in the field. The median value was found after each measurement was made at least three times.

### Statistical Analysis

Data were analyzed using SPSS 22 (SPSS Inc., Chicago, IL, USA) program. First, the Shapiro Wilks test was used to determine the appropriateness of the

variables to the normal distribution. Next, Spearman's Rho test was used to correlate USG values within the groups at the beginning of the experiment. Finally, Nonparametric Kruskal Wallis and Mann Whitney U tests were used to determining a significant difference between the USG and HP measurements in these four groups. P-value <0.05 was considered statistically significant.

For interobserver reliability, the intraclass correlation coefficient (Intraclass Correlation Coefficient) test was used. The intraclass correlation coefficient is divided into five groups. These groups were accepted as 0-0.2 poor, 0.21-0.4 average, 0.41-0.6 fair, 0.61-0.8 good and 0.81-1 excellent (23).

## RESULTS

The inter-observer correlation was 0.99 (Intraclass Correlation Coefficient test).

### Ultrasound Measurements

IMT measurements of right CCA left CCA, AA, IA, and right kidney RI measurements are given in the Table 2.

End of the experiment in the EE group, statistically significant increase was found in the USG measurements of rCCA, ICCA, AA and IA IMT ( $p = 0.001$ ,  $p = 0.001$ ,  $p = 0.018$ ,  $p = 0.008$ , respectively), compared to the sham group.

End of the experiment in the LE group, a statistically significant increase was found in IMT measurements performed by USG in the rCCA, ICCA, AA, and IA ( $p=0,001$ ,  $p=0,001$ ,  $p=0,003$ ,  $p=0,001$ , respectively), in comparison to the sham group. In addition to these findings, rRI increased significantly in the LE group at the end of the experiment ( $p = 0.038$ ).

### Histopathological Measurements

In EE group, HP evaluation of IMT in the rCCA, ICCA, AA and IA also showed statistically significant increase, compared to the sham group ( $p=0,035$ ,  $p=0,001$ ,  $p=0,014$ ,  $p=0,008$ , respectively).

In the LE group, statistically significant increase was found in the rCCA, ICCA, AA and IA IMT measurements performed by HP, compared to the sham group ( $p=0,008$ ,  $p=0,005$ ,  $p=0,005$ ,  $p=0,008$ , respectively).

There was no statistically significant increase or decrease in serum eNOS, ADMA, VEGF levels, and tissue eNOS and ET-1 levels in the EE and LE groups at the beginning and end of the experiment ( $p > 0.05$ ).

## DISCUSSION

In this study, we created a full-body, noninvasive ultrasonography model for AS and ED experiments in rats. Thanks to this new model, anatomical structures that can be looked at for various parts of the body in rat experiments were defined.

Demonstration of ED and AS is carried out by the gold standard HP and blood and urine analysis methods because it is relatively more accessible. However, due to the invasive nature of these methods, the use of imaging systems is required. Thanks to technological advances, the place of ultrasonography in small animal experiments are increasing day by day.

The literature on ED and AS has focused either on a single tissue (18) or vessels associated with the disease of interest (17). The use of arteries in different sections in different experiments causes failure to create a standard model for the whole body in experimental models. Our study has enabled ED to be defined by USG more holistically and comprehensively by showing ED in vessels of different anatomical localization and the right kidney. In this way, a model has emerged that can vary according to the planned model and can be made other provisions.

The two practitioners who make the measurements are quite experienced in IMT measurements in experimental animals. Therefore, the inter-observer correlation was found to be perfect. The fact that they have worked together in previous studies has made the method quite standard. The high inter-observer correlation shows that the method described, and the measurements made are not affected by the difference between the observers.

The fact that the experimental initial USG measurements in the sham, EE, and LE groups are not different indicates that the rats have similar tissues.

Histopathological measured IMT is less than USG measurements. This may be due to the shrinkage of surgically removed tissue in the chemical substance, as previously described (24). However, even in this case, the statistically significant similarities of the change between HP and USG measured IMTs show how valuable USG measurements are.

The differences in IMT values of vessels defined in EE and LE groups at the end of the experiment, within the group, and in the sham group comparisons indicate that ED and AS developed due to N-Nitro-L-Arginine Methyl Ester Hydrochloride. Furthermore,

the fact that there was no change in sham group measurements at the end of the experiment enabled us to understand that predicted, and unforeseen factors such as aging and injection did not affect the experiment. In this way, the N-Nitro-L-Arginine Methyl Ester Hydrochloride effect could be demonstrated by USG and by HP.

It is known that the morphological findings that develop due to ED increase over time. HP evaluation of renal interlobar arteries and mesenteric arteries predicts renal damage in hypertensive rats (25). Kidney RI measurement successfully shows hypertension and "end-organ" damage of AS (26). It has been demonstrated that RI values increase in the case of kidney damage in rats and that RI measurement can be used to diagnose kidney function (27). In our study, the increase of this value in the LE group indicates the end-organ finding of the effects that develop due to ED. We think that the change in the RI value of the kidney within the group, but not in the EE group, due to the short duration of the hypertensive effect and the absence of kidney damage that may develop due to this.

Showing ED by imaging not only in the vascular system but also in the kidney RI increases the depth of the model. This increase was not statistically significant compared to the sham group, and HP could not examine the kidney tissue reveals the need for more experiments on this subject. There have been deficiencies in demonstrating the diagnosis of ED with biochemical methods. This situation has developed due to the difficulties experienced by the relevant laboratory in the supply of personnel and materials during the pandemic process. In addition, in the parts of the experiment that coincided with the pandemic process, it was difficult for the researcher to reach the laboratory to apply the biochemical tests, and clotting occurred in some blood samples. Therefore, biochemical verification of ED and AS has not been successful. Nevertheless, the detection of USG findings like HP, which is the gold standard diagnosis of ED and AS, reveals its importance in imaging small animal experiments.

Our most important limitation is that only one pathologist looks at the tissues in our study. Another limitation is that kidney tissues were not examined by HP.

## CONCLUSION

In small animal experiments where ED and AS were studied, an inclusive and whole-body diagnostic

noninvasive model was created for the first time with ultrasonography. Measurement of renal RI value in ED and AS models is a promising new method for diagnosis.

**Acknowledgement:** List all contributors who do not meet the criteria for authorship, such as technical assistants, writing assistants or head of department who provided only general support.

**Author contribution:** Design: MKS, OY, ZSA, SA, MS Data Collection: MKS, MMB, OY, YC, SB Interpretation: MKS, MB, YC Writing: MKS, MMB, YC, SB.

**Conflict of interests:** The authors have no conflicts of interest to declare.

**Ethical approval:** Dokuz Eylul University Animal Care and Use Ethical Committee approved all animal protocols (Date: 14.07.2018. Number: 37 / 2018).

**Funding** None.

**Peer-review:** Externally peer-reviewed.

## REFERENCES

1. Topol, E.J. and R.M. Califf, Textbook of cardiovascular medicine. 2007: Lippincott Williams & Wilkins.
2. Onat, A., Risk factors and cardiovascular disease in Turkey. *Atherosclerosis*, 2001. 156(1): p. 1- 10.
3. Glagov, S., et al., Compensatory enlargement of human atherosclerotic coronary arteries. *New England Journal of Medicine*, 1987. 316(22): p. 1371-1375.
4. Ibañez, B., J.J. Badimon, and M.J. Garcia, Diagnosis of atherosclerosis by imaging. *The American journal of medicine*, 2009. 122(1): p. S15-S25.
5. Playford, D.A. and G.F. Watts, Special article: non-invasive measurement of endothelial function. *Clin Exp Pharmacol Physiol*, 1998. 25(7-8): p. 640-3.
6. Takase, B., et al., Endothelium-dependent flow-mediated vasodilation in coronary and brachial arteries in suspected coronary artery disease. *Am J Cardiol*, 1998. 82(12): p. 1535-9, a7-8.
7. Schroeder, S., et al., Noninvasive determination of endothelium-mediated vasodilation as a screening test for coronary artery disease: pilot study to assess the predictive value in comparison with angina pectoris, exercise electrocardiography, and myocardial perfusion imaging. *Am Heart J*, 1999. 138(4 Pt 1): p. 731-9.
8. Schächinger, V., M.B. Britten, and A.M. Zeiher, Prognostic impact of coronary vasodilator dysfunction on adverse long-term outcome of coronary heart disease. *Circulation*, 2000. 101(16): p. 1899-1906.
9. Suwaidi, J.A., et al., Long-term follow-up of patients with mild coronary artery disease and endothelial dysfunction. *Circulation*, 2000. 101(9): p. 948-54.
10. Faulx, M.D., A.T. Wright, and B.D. Hoit, Detection of endothelial dysfunction with brachial artery ultrasound scanning. *Am Heart J*, 2003. 145(6): p. 943-51.
11. Woo, K., et al., Overweight in children is associated with arterial endothelial dysfunction and intima-media thickening. *International journal of obesity*, 2004. 28(7): p. 852-857.
12. Järvisalo, M.J., et al., Increased aortic intima-media thickness: a marker of preclinical atherosclerosis in high-risk children. *Circulation*, 2001. 104(24): p. 2943-2947.
13. Xiangdong, L., et al., Animal models for the atherosclerosis research: a review. *Protein & cell*, 2011. 2(3): p. 189-201.
14. Khayyal, M.T., et al., Blood pressure lowering effect of an olive leaf extract (*Olea europaea*) in L-NAME induced hypertension in rats. *Arzneimittelforschung*, 2002. 52(11): p. 797-802.
15. Pechanova, O., et al., Red wine polyphenols prevent cardiovascular alterations in L-NAME-induced hypertension. *J Hypertens*, 2004. 22(8): p. 1551-9.
16. Pignoli P, Tremoli E, Poli A, Oreste P, Paoletti R Intimal plus medial thickness of the arterial wall: a direct measurement with ultrasound imaging. *Circulation*, 1986 Dec; 74(6):1399-406.
17. Park, K., et al., Initial validation of a novel rat model of vasculogenic erectile dysfunction with generalized atherosclerosis. *International journal of impotence research*, 2005. 17(5): p. 424- 430.
18. Wang, H.-t., et al., Guidelines for assessing mouse endothelial function via ultrasound imaging: a report from the International Society of Cardiovascular Translational Research. *Journal of cardiovascular translational research*, 2015. 8(2): p. 89-95
19. Kemmner S, Lorenz G, Wobst J, Kessler T, Wen M, Günthner R, Stock K, Heemann U, Burkhardt K, Baumann M, Schmaderer C. Dietary nitrate load lowers blood pressure and renal resistive index in patients with chronic kidney disease: A pilot study. *Nitric Oxide*. 2017 Apr 1; 64:7-15. doi: 10.1016/j.niox.2017.01.011. Epub 2017 Jan 28. PMID: 28137609.
20. Sugiura T, Nakamori A, Wada A, Fukuhara Y. Evaluation of tubulointerstitial injury by Doppler

- ultrasonography in glomerular diseases. Clin Nephrol. 2004 Feb;61(2):119-26. doi: 10.5414/cnp61119. PMID: 14989631.
21. Ikee R, Kobayashi S, Hemmi N, Imakiire T, Kikuchi Y, Moriya H, Suzuki S, Miura S. Correlation between the resistive index by Doppler ultrasound and kidney function and histology. Am J Kidney Dis. 2005 Oct;46(4):603-9. doi: 10.1053/j.ajkd.2005.06.006. PMID: 16183414.
  22. Bigé N, Lévy PP, Callard P, Faintuch JM, Chigot V, Jousselin V, Ronco P, Boffa JJ. Renal arterial resistive index is associated with severe histological changes and poor renal outcome during chronic kidney disease. BMC Nephrol. 2012 Oct 25; 13:139. doi: 10.1186/1471-2369-13-139. PMID: 23098365; PMCID: PMC3531254.
  23. Aktürk, Zekeriya, and Hamit Acemoğlu. "Tıbbi araştırmalarda güvenilirlik ve geçerlilik." *Dicle Tıp Dergisi* 39.2 (2012): 316-319.
  24. Gan, L.-m., et al., Non-invasive real-time imaging of atherosclerosis in mice using ultrasound biomicroscopy. *Atherosclerosis*, 2007. 190(2): p. 313-320.
  25. Sohn, E.J., et al., Effect of methanol extract of *Sorbus cortex* in a rat model of L-NAME-induced atherosclerosis. *Biol Pharm Bull*, 2005. 28(7): p. 1239-43
  26. Pontremoli, R., et al., Increased renal resistive index in patients with essential hypertension: a marker of target organ damage. *Nephrology, dialysis, transplantation: official publication of the European Dialysis and Transplant Association-European Renal Association*, 1999. 14(2): p. 360-365.
  27. Karakus, S., et al., The effect of enalapril on renal resistive index, urine electrolyte levels and tgf- $\beta$ 1 levels of kidney tissues in rats with unilateral partial ureteropelvic junction obstruction. *European Journal of Pediatric Surgery*, 2011. 21(06): p. 356-361